Dalton Transactions

Accepted Manuscript

ROYAL SOCIETY OF CHEMISTRY

www.rsc.org/dalton

Synthesis, characterisation and antibacterial activity of [(*p*-cym)RuX(L)]$^{+/2+}$ (X= Cl, H_2O; L = bpmo, bpms) complexes

Suman Kumar Tripathy,[a] Ashoka Charry Taviti,[b] Niranjan Dehury,[a] Anupam Sahoo,[a] Satyanaryan Pal[c] Tushar Kant Beuria,[*b] and Srikanta Patra[*a]

[a]*School of Basic Sciences, Indian Institute of Technology Bhubaneswar, Bhubaneswar, Odisha - 751007, India.*

[b]*Institute of Life Science, Bhubaneswar, Odisha - 751007, India.*

[c]*Department of Chemistry, Ravenshaw University, Cuttack -753 003, Odisha, India.*

Abstract

Mononuclear half sandwiched complexes [(*p*-cym)RuCl(bpmo)](ClO_4) {[**1**](ClO_4)} and [(*p*-cym)RuCl(bpms)](PF_6) {[**2**](PF_6)} have been prepared by reacting heteroscorpionate ligands bpmo = 2-methoxyphenyl-bis(3,5-dimethylpyrazol-1-yl)methane and bpms = 2-methylthiophenyl-bis(3,5-dimethylpyrazol-1-yl)methane, respectively, with dimeric precursor complex [(*p*-cym)RuCl(μ-Cl)]$_2$ (*p*-cym = 1-isopropyl-4-methylbenzene) in methanol. The corresponding aqua derivatives [(*p*-cym)Ru(H_2O)(bpmo)](ClO_4)$_2$ {[**3**](ClO_4)$_2$} and [(*p*-cym)Ru(H_2O)(bpms)](PF_6)$_2$ {[**4**](PF_6)$_2$} are obtained from {[**1**](ClO_4)} and {[**2**](PF_6)}, respectively, *via* Cl^-/H_2O exchange process in presence of appropriate equivalents of $AgClO_4/AgNO_3$+KPF_6 in methanol-water mixture. The molecular structures of complexes {[**1**]Cl, [**3**](ClO_4)$_2$ and [**4**](PF_6)(NO_3)} are authenticated by their single crystal X-ray structures. The complexes have shown expected piano-stool geometry with *p*-cym in η^6 binding mode. The aqua complexes [**3**](ClO_4)$_2$ and [**4**](PF_6)$_2$ show significantly good antibacterial activity towards *E. coli* (gram negative) and *B. subtilis* (gram positive) strains, while chloro derivatives ({[**1**](ClO_4)} and {[**2**](PF_6)} are found to be virtually inactive. The order of antibacterial activity of the complexes according to their MIC values are [**1**](ClO_4) (both 1000 μg/mL) < [**2**](PF_6) (580 μg/mL and 750 μg/mL) < [**3**](ClO_4)$_2$ (both 100 μg/mL) < [**4**](PF_6)$_2$ (30 μg/mL and 60 μg/mL) for both *E. coli* and *B. subtilis* strains, respectively. Further, the aqua complexes [**3**](ClO_4)$_2$ and [**4**](PF_6)$_2$ have shown clear zones of inhibition against kanamycin, ampicillin and chloramphenicol resistant *E.coli* strains. The detailed mechanistic aspects of the aforesaid active aqua complexes [**3**](ClO_4)$_2$ and [**4**](PF_6)$_2$ have been explored and it reveals that both the complexes inhibit the number of nucleoid per cell *in vivo* and bind to DNA *in vitro*. The results

indeed demonstrate that both [**3**]$(ClO_4)_2$ and [**4**]$(PF_6)_2$ facilitate the inhibition of bacterial growth by binding to DNA.

Introduction

Bacterial resistance is one of the major concerns in the developing world which contributes considerably towards the human mortality rate.[1] In every coming days bacteria are gaining resistance against the known antibiotics and thus making the treatment ineffective.[1a, 2] This necessitates the development of new class of antibacterial agents which can show better activity or alternative mode of action as compared to the existing ones. Metal complexes could be a suitable choice to overcome the challenges.[3] Metal complexes often provide tunable parameters such as variable oxidation states, coordination number and geometry. In addition, by simple variation of ligands and metal centers the desired chemical and biological activities of the metal complexes can be fine-tuned. Accordingly, a large number of metal complexes of iron, silver, zinc, cobalt, copper, nickel, iridium, etc. have been developed and studied their antibacterial activities.[3c, 4]

Among various metals, ruthenium complexes possess relatively higher stability under various physiological conditions.[1b, 5] Hence, ruthenium complexes have greatly been used to study the anticancer activity,[6] antibacterial activity,[7] DNA and protein binding[8] in addition to their common applications in catalysis[9] and chemiluminescence.[10] Keene and Collins *et al*. have conducted extensive research for the development of ruthenium polypyridyl complexes as antibacterial agents.[7a, c, d, 8e, 11] Many of their compounds are demonstrated to participate in killing multidrug resistant bacteria *Staphylococcus aureus*.[8e, 11a, c] Further, Smith *et al.* have also reported efficient antimalarial activity of ruthenium(II) complexes against chloroquine-resistant parasite *Plasmodium falciparum*.[6g, 7e, 11c, 12] Recently, Wong, Gambari, Lee and Li *et al* have

shown the excellent antibacterial activity with low toxicity of ruthenium bipyridyl based complexes.[1b] Although the arene ruthenium complexes have been used as anticancer agents, study of their antibacterial activities have not been explored in detail.[13] Further, much attention has not been paid to the development and biological activity of arene ruthenium complexes of bis(pyrazol-1-yl)methane based heteroscopionate ligands, though they are considered to be an excellent class of ligands in terms of their spectator nature and tunable steric and electronic parameters. Recently, we have demonstrated that replacement of Cl^- by H_2O in (chloro)bis(pyrazol-1-yl)methane based η^6 arene ruthenium(II)complexes significantly enhanced their anticancer activity.[6a] In this context the present article intends to highlight the development of mononuclear arene ruthenium(II) complexes encompassing bis(pyrazol-1-yl)methane based heteroscorpionate ligands and their potential application in antibacterial activity.

Herein, we report the synthesis and characterisation of mononuclear chlorido complexes [(*p*-cym)RuCl(bpmo)](ClO_4) {[**1**](ClO_4)} and [(*p*-cym)RuCl(bpms)](PF_6) {[**2**](PF_6)} and their corresponding aqua derivatives [(*p*-cym)Ru(H_2O)(bpmo)](ClO_4)$_2$ {[**3**](ClO_4)$_2$} and [(*p*-cym)Ru(H_2O)(bpms)](PF_6)$_2$ {[**4**](PF_6)$_2$} incorporating 2-methoxyphenyl-bis(3,5-dimethylpyrazol-1-yl)methane (bpmo) and 2-methylthiophenyl-bis(3,5-dimethylpyrazol-1-yl)methane (bpms) ligands. The structural features and spectroscopic properties of the complexes have been studied by various analytical and spectroscopic techniques. The antibacterial activity of the complexes towards *E. coli* (gram negative) and *B. subtilis* (gram positive) strains and mechanistic details of bacterial cell death have also been scrutinised using different microbial, biochemical and microscopic techniques.

Results and discussion

Synthesis and spectral aspects

The ligands 2-methoxyphenyl-bis(3,5-dimethylpyrazol-1-yl)methane (bpmo) and 2-methylthiophenyl-bis(3,5-dimethylpyrazol-1-yl)methane (bpms) have been prepared by slight modification of the reported procedure.[14] The mononuclear chlorido complexes [**1**]ClO_4 and [**2**](PF_6) have been prepared by reacting bpmo and bpms ligands, respectively, with the dimeric precursor $[(p\text{-cym})RuCl(\mu\text{-}Cl)]_2$ in 2:1 mole ratio in refluxing methanol under aerobic reaction condition and isolated as their ClO_4^-/PF_6^- salt. The corresponding aqua derivatives [**3**]$(ClO_4)_2$ and [**4**]$(PF_6)_2$ are obtained by Cl^-/H_2O exchange reaction in the presence of $AgClO_4/AgNO_3$+KPF_6 in water-methanol mixture (Scheme 1). The complexes are air stable and have shown reasonably good solubility in most of the polar solvents. The synthesis and ^1H NMR characterisation of BF_4^- salt of $\mathbf{1}^+$ is reported elsewhere; however, the structural, spectral and electrochemical properties as well as its anticancer or antimicrobial activities have not yet been studied.[15]

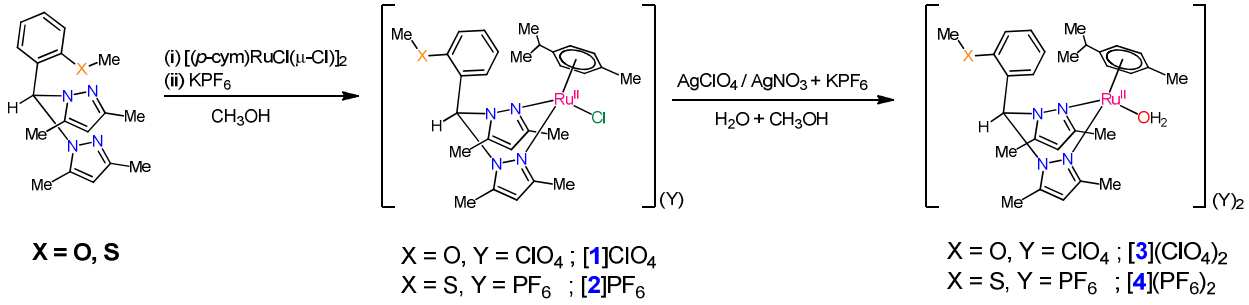

Scheme 1. Synthetic outline for the complexes [**1**](ClO_4) - [**4**]$(PF_6)_2$.

The chlorido complexes [**1**](ClO_4), [**2**](PF_6) and their aqua derivative [**3**]($ClO_4)_2$, [**4**]$(PF_6)_2$ behave as 1:1 and 1:2 electrolytes in solution, respectively, and give satisfactory microanalytical data (See Experimental Section). The presence of ClO_4^- and PF_6^- counter anions in the complexes has been evidenced by the characteristic IR vibrations at 1100 cm^{-1} and 625 cm^{-1} for $\nu(ClO_4^-)$ and 845 cm^{-1} for $\nu(PF_6^-)$. The molecular ion peaks centred at 581.27 for $\{[\mathbf{1}](ClO_4) - ClO_4\}^+$ (calcd. 581.14), 597.24 for $\{[\mathbf{2}](PF_6) - PF_6\}^+$ (calcd. 597.20), 645.10 for $\{[\mathbf{3}](ClO_4)_2 - ClO_4 - H_2O\}^+$ (Calcd. 645.14) and 723.94 for $\{[\mathbf{4}](PF_6)_2 - PF_6\}^+$ (Calcd. 723.12) are detected in their +ve ion ESI mass spectra in CH_3OH, supporting their identities in solution (Fig. 1). The ^1H NMR spectra of the complexes in DMSO-d_6 exhibit expected number of proton resonance within the chemical shift range 0 - 10 ppm indicating the presence of *p*-cym and bis(pyrazol-1-yl)methane based ligands. The ^1H NMR signal for the coordinated H_2O of [**3**]$(ClO_4)_2$ and [**4**]$(PF_6)_2$ are not resolved, possibly due to rapid $H_2O/(CD_3)_2SO$ exchange process at NMR time scale.

The electronic spectra of the complexes are recorded in CH_3CN (Fig. S1). The chlorido complexes [**1**](ClO_4) and [**2**](PF_6) exhibit MLCT/d-d bands at 420 nm and 416 nm, respectively, in addition to multiple intra-ligand charge transfer bands in the UV region.[16] On switching from the chlorido complexes to their corresponding aqua derivatives [**3**]$(ClO_4)_2$ and [**4**]$(PF_6)_2$, the MLCT band blue shifted to 395 nm with little change in intensity due to the stronger ligand field strength of H_2O as compared to that of Cl^- ligand.[6a, 15, 17]

Structural aspects

The identities of complexes [**1**]Cl, [**3**]$(ClO_4)_2$ and [**4**]$(PF_6)(NO_3)$ are further confirmed by single crystal X-ray crystallography (Fig. 2). Complex [**1**]Cl crystallises in monoclinic space group *P21/n* whereas complexes [**3**]$(ClO_4)_2$ and [**4**]$(PF_6)(NO_3)$ crystallise in triclinic space group P–*1*. Selected crystallographic parameters and important bond lengths and bond angles are set in

Tables 1 and 2, respectively. The single crystal of [**1**]Cl contains $2H_2O$ molecules per unit cell. The distorted octahedral geometries of [**1**]Cl, [**3**]$(ClO_4)_2$ and [**4**]$(PF_6)(NO_3)$ have been revealed by the angles imposed around the metal centres. The complexes exhibit expected three-legged piano stool geometry with *p*-cym ligand with an average Ru-$C_{centroid}$ distance of 1.713 Å for [**1**]Cl, 1.695 Å for [**3**]$(ClO_4)_2$ and 1.694 Å for [**4**]$(PF_6)(NO_3)$. The remaining coordination sites of the metal centres are occupied by a bidentate nitrogen donor bis(pyrazolyl-1-yl)methane and a chloride for [**1**]Cl and water for [**3**]$(ClO_4)_2$ and [**4**]$(PF_6)(NO_3)$. The bidentate bis(pyrazolyl-1-yl)methane yields a six membered metallacycle, adopting a boat conformation with a N1-Ru1-N3, N1-Ru1-N4 and N1-Ru1-N3 bite angles of 84.4(2)^o for [**1**]Cl, 85.82(9)^o for [**3**]$(ClO_4)_2$ and 85.63(12)^o for [**4**]$(PF_6)(NO_3)$, leaving the methoxyphenyl or thiomethoxyphenyl group uncoordinated. The dihedral angle between the pyrazolyl rings is 55.74^o for [**1**]Cl, 53.74^o for [**3**]$(ClO_4)_2$ and 56.21^o for [**4**]$(PF_6)(NO_3)$. The observed Ru-N bond distances, 2.138 Å - 2.143 Å for [**1**]Cl, 2.12 Å - 2.133 Å for [**3**]$(ClO_4)_2$ and 2.129 Å -2.137 Å for [**4**]$(PF_6)(NO_3)$ are in good agreement with the previously reported complexes.[6a, 18] The Ru-O bond distances 2.141 Å for [**3**]$(ClO_4)_2$ and 2.125 Å for [**4**]$(PF_6)(NO_3)$ are close to the values reported for structurally characterised other {Ru-(*p*-cym)} based aqua complexes.[6a] However, the Ru-Cl bond distance of 2.427Å for [**1**]Cl is slightly longer as compared to that in the related reported complexes.[6a, 9b, 19]

Electrochemical properties

The cyclic voltammetric studies of the complexes have been performed in CH_3CN at room temperature using saturated calomel reference electrode (SCE) and glassy carbon working electrode. The representative cyclic voltammograms are shown in Fig. S2. Complexes [**1**](ClO_4) and [**2**](PF_6) exhibit irreversible Ru^{II}/Ru^{III} oxidation processes, E_{pa} at 0.88 V and 0.78 V, respectively. This oxidation is significantly lowered (~ 300mV) as compared to the previously

reported mononuclear [(*p*-cym)RuCl(pz_4lut)]Cl complexes which can be attributed to the electron donating nature of the methoxyphenyl or thiomethoxyphenyl group present in the bis(pyrazol-1-yl)methane framework.[6a] In addition, both complexes have shown an additional irreversible oxidation peak E_{pa} at 1.43 V and that could be assigned as Ru^{III}/Ru^{IV} oxidation process. Both the complexes have shown multiple irreversible ligand based reductions at -0.96V, -1.10V and -1.80V for [**1**](ClO_4) and -0.83V, -1.16V and -1.93V for [**2**](PF_6). Unfortunately, we failed to detect any reasonable electrochemical response for [**3**](ClO_4)$_2$ and [**4**](PF_6)$_2$ in both water and acetonitrile in spite of our repeated attempts. This could be due to the much higher stabilisation of the ruthenium (II) state in the aqua complexes as compared to their chlorido derivatives.[6a, 18]

Complex-DNA interaction studies

Arene ruthenium complexes are well known for their interaction with DNA. To check the interaction of the synthesised complexes with DNA ethidium bromide (EB) displacement experiment using fluorescent spectroscopy has been conducted. It is well known that EB efficiently intercalate with DNA helix and become strong emitter during intercalation with DNA on excitation at 520 nm.[8a]

The fluorescence intensity of EB-DNA adduct can be decreased by addition of quencher. This arises due the decrease of available number of binding site on the DNA for EB and presumably because of the competition with complexes which is non-emissive under that experimental condition. The displacement of EB from EB – calf thymus DNA (CT DNA) adduct with complexes [**1**](ClO_4) - [**4**](PF_6)$_2$ is shown Fig. S3. It is observed that increasing the concentration of complexes causes the decrease in fluorescence intensity at 598 nm indicating the interaction of

the complexes with CT DNA.[8a, 20] The magnitude of interaction of the complexes with CT DNA has been assayed quantitatively by using Stearn–Volmer equation (eq. 1).

$$F_0/F = 1 + K_{SV}[Q] \qquad \text{eq 1}$$

Where F_0 and F are the fluorescence intensity of EB - CT DNA adduct before and after the addition of complexes, K_{SV} is the Stern-Volmer constant, and [Q] is the concentration of the desired complex added. The K_{SV} values calculated from the slope of plot F_0/F *vs* [Q] (Fig. S3 inset) are 1.12 x 10^4 M^{-1}, 1.4 x 10^4 M^{-1}, 1.68 x 10^4 M^{-1} and 2.0 x 10^4 M^{-1} for the complexes [**1**](ClO_4) - [**4**]$(PF_6)_2$, respectively. The apparent binding constant also have been evaluated by using the equation 2.

$$K_{app} = K_{EB}[EB]/[Q]_{50\%} \qquad \text{eq 2}$$

Where K_{app} is the apparent binding constant, K_{EB} binding constant of EB to CT DNA, and $[Q]_{50\%}$ is the concentration of complexes at the 50% of initial fluorescence intensity. The apparent binding constant for complexes [**1**](ClO_4) - [**4**]$(PF_6)_2$ are found to be 3.7 x 10^4 M^{-1}, 4.5 x 10^4 M^{-1}, 5.9 x 10^4 M^{-1} and 7.5 x 10^4 M^{-1}, respectively (K_{EB} = 1.0 x10^7 M^{-1}). The above results indicate moderately strong interaction of the complexes with CT DNA and the aqua complexes ([**3**]$(ClO_4)_2$ and [**4**]$(PF_6)_2$) show better binding affinity than their corresponding chlorido analogues ([**1**](ClO_4) and [**2**](PF_6)).

Further, to understand the binding mode of complexes with CT DNA hydrodynamic measurements using Ostwald Viscometer has been conducted. Viscosity measurement of CT DNA in the presence and absence of metal complexes has shown the enhancement of relative viscosity with increase in concentration of complexes, indicating the intercalative binding of the complexes with CT DNA (Fig. S4).[20]

Antibacterial activity

To explore the antibacterial potency of the complexes, *E. coli*Bl21 and *B. subtilis*168 strains are used in the present study. The antibacterial properties of the complexes are monitored using a growth curve and disc diffusion assay. The overnight cultures of both bacteria have been diluted to OD_{600} ~ 0.1 and grown in the absence and presence (200 µg/mL) of complexes. The growth curves have been drawn by monitoring the absorbance at 600 nm over a period of 6 h with an interval of 1 h (Fig. 3). No significant growth inhibition of both *E. coli or B. subtilis* strains is observed during the treatment of complexes [**1**](ClO_4) and [**2**](PF_6), however, it is inhibited completely for [**3**]$(ClO_4)_2$ and [**4**]$(PF_6)_2$(Fig. 3). To further confirm the antibacterial activity of the complexes disc diffusion assay has been conducted. All complexes are found to be active at the concentration level of 100 µg/mL, however, the aqua complexes have shown higher growth inhibition towards both *E. coli* and *B. subtilis* strains with significant zones of inhibition (Table 3). Furthermore, the MIC values have been determined using the procedure mentioned in the experimental section. The order of MIC values of the complexes against *E. coli* and *B. subtilis* strains are [**4**]$(PF_6)_2$ > [**3**]$(ClO_4)_2$ > [**2**](PF_6) > [**1**](ClO_4) which are in consonance with the results observed in growth curve experiments (Table 3). Thus, both the assays together suggest that the aqua complexes are more active as compared to their chlorido analogues. Hence, complexes [**3**]$(ClO_4)_2$ and [**4**]$(PF_6)_2$ have been chosen for further studies.

To test whether the complexes [**3**]$(ClO_4)_2$ and [**4**]$(PF_6)_2$ are effective against resistant bacterial strains; kanamycin, ampicillin and chloramphenicol resistant *E.coli* strains have been used. Both [**3**]$(ClO_4)_2$ and [**4**]$(PF_6)_2$ have shown clear zones of inhibition against the resistant bacterial strains similar to the control non-resistant *E. coli* (Fig. 4). The results indicate that the mode of action of the complexes [**3**]$(ClO_4)_2$ and [**4**]$(PF_6)_2$ towards *E. coli* strains is different from that of

kanamycin, ampicillin and chloramphenicol. This indeed prompted us to investigate the mode of action of these complexes. The inhibition of bacterial growth may happen *via* the alterations in cell morphology, perturbation of membrane structures or the disorder in nucleoid structure. To get more insight into the above parameters fluorescence and differential interference contrast (DIC) microscopic investigations have been conducted for both *E. coli* and *B. subtilis*. The bacteria membrane and nucleoid have been stained with the dye FM4-64 and DAPI, respectively. The fluorescence microscopic images have shown clear membrane structure and a nicely shaped nucleoid with normal cell morphology of both the bacterial strains in the absence of complexes [**3**]$(ClO_4)_2$ and [**4**]$(PF_6)_2$ (Figs. 5A and S5A). However, the total number of bacteria has reduced significantly in the presence of [**3**]$(ClO_4)_2$ and [**4**]$(PF_6)_2$ which is consistent with our previous observations. Further, the FM4-64 stained images have shown the malformed cell membranes as compared to the control cells which is lysed at many places. To confirm this the Propidium Iodide (PI) staining of the *E. coli* nucleoid has been performed. PI will stain the nucleoids only in the case where the membranes are ruptured. None of the control cells were stained by PI showing that the membranes of the *E. coli* are fully intact. However most of the cell in the presence of complexes [**3**]$(ClO_4)_2$ or [**4**]$(PF_6)_2$ were stained by PI indicating the membranes were ruptured and partially lysed in the presence of the ruthenium complexes (Fig 5B). In addition, properly shaped nucleoid is also absent in most of the cells treated with both the complexes. Based on the observations, the following four parameters such as cell length, membrane structure, number of nucleoids and nucleoid structure for each of the cells in the presence and absence of complexes [**3**]$(ClO_4)_2$ and [**4**]$(PF_6)_2$ have been determined (Figs. 5C and S5B). It is observed that although the average length of the cell has not changed much, most of the treated cells are devoiding proper membranes and right numbers or correct shaped nucleoids (Figs. 5C

and S5B). These results collectively suggest that the complexes [**3**]$(ClO_4)_2$ and [**4**]$(PF_6)_2$ kill the bacteria by perturbing nucleoid structures. The planner arene compounds are known to interact with the DNA by intercalation which further supports our observations.

To gain more insight into the mechanism we have studied the interactions of the complexes [**3**]$(ClO_4)_2$ and [**4**]$(PF_6)_2$ with DNA. An electrophoretic mobility shift assay (EMSA) has been performed with a 267 bp DNA as described in the experimental section. The DNA band has shifted upward in the presence of complexes [**3**]$(ClO_4)_2$ and [**4**]$(PF_6)_2$ and the shift increases with the increase in concentrations of the complexes. (Fig. 6A). In addition, the intensity of gel band is reduced with the increasing concentration of both the complexes, indicating that the complexes have replaced ethidium bromide (EB), a known strong DNA intercalating agent, from the DNA. This suggests that the complexes [**3**]$(ClO_4)_2$ and [**4**]$(PF_6)_2$ bind with the DNA either by a similar mechanism as EB or make conformational change that prevents the binding of EB to DNA. To further confirm the interaction of the complexes with DNA, the restriction digestion of a purified plasmid vector (pZs-green, Invitrogen) with NdeI restriction enzyme in the presence and absence of EB or complexes [**3**]$(ClO_4)_2$ and [**4**]$(PF_6)_2$ has been performed. In the absence of compounds, NdeI digests the plasmid DNA and a fragment of 672 bp has come out (Fig 6B). In the presence of EB (5 μM) the NdeI, digestion is inhibited nearly by half, however, in the presence of 10 μg of [**3**]$(ClO_4)_2$ and [**4**]$(PF_6)_2$ the NdeI digestion is inhibited completely. This results is consistent with the results observed in EB displacement assay and viscosity measurements. Thus, the results collectively suggest that both the aqua complexes bind to DNA with a strong affinity and the antibacterial activity of the complexes may be derived from their interaction to the bacterial DNA.

Conclusion

In conclusion, the present article highlights the synthesis, characterisation and antibacterial activity of mononuclear arene ruthenium(II) complexes [**1**](ClO_4) - [**4**]($(PF_6)_2$ derived from bis(pyrazol-1-yl)methane based heteroscorpionate ligands (bpmo and bpms). The complexes have shown moderately strong interaction with CT DNA evidenced from the EB displacement assay and viscosity measurement experiments. Moreover, the aqua complexes have shown higher antibacterial activity against both *E. coli* and *B. subtilis* strains than their chlorido analogues. The order of antibacterial activity are found to be [**4**]$(PF_6)_2$ > [**3**]$(ClO_4)_2$ > [**2**](PF_6) > [**1**](ClO_4). Further, the aqua complexes have shown comparatively good activity against kanamycin, ampicillin and chloramphenicol resistant *E.coli* strains. The detailed mechanistic aspects of the active aqua complexes have been explored using microscopic analysis, electrophoretic mobility shift assay (EMSA) and restriction digestion assay. The studies reveal that both the aqua complexes inhibit the number of nucleoid per cell *in vivo* and bind to DNA *in vitro* and kill bacteria by perturbing nucleoid structures. Although the arene ruthenium complexes are well established as anticancer agents but their antibacterial efficacy is not well examined. Even though the antibacterial activity of present set of complexes are not significantly high, the detailed mechanistic investigation and their activity against resistant strains extending the scope of further research. Thus, we believe that our findings may provide significant impetus in designing and developing heteroscorpionate ligand based η^6-arene-ruthenium (II) complexes for further biomedical applications as antibacterial agents.

Experimental

Materials

The starting complex [Ru(*p*-cym)Cl(μ-Cl)]$_2$[21] was prepared by following the reported procedure. The ligands 1,1'-((2-methoxyphenyl)methylene)bis(3,5-dimethyl-1H-pyrazole) (bpmo) and1,1'-((2-(methylthio)phenyl)methylene)bis(3,5-dimethyl-1H-pyrazole) (bpms) was prepared by adopting slight modification of the reported procedures.[14] Ampicillin, Kanamycin, Chloramphenicol and DMSO were obtained from Sigma-Aldrich, USA; LB broth, LB agar, Filter discs and Petri plates were obtained from Himedia, India. DAPI and FM4-64 were purchased from Life technology. All other chemicals were purchased from commercial sources and used as received. Solvents were dried by conventional methods and distilled prior to use.

Instrumentation

UV-Vis spectra were recorded by using a Perkin Elmer Lambda 35 spectrophotometer. FTIR spectra were obtained using Bruker Alpha FTIR spectrophotometer with samples prepared as KBr pellets. Solution electrical conductivity was checked using OKATON PC 2700 Conductivity bridge. Elemental analyses were carried out using EuroVector elemental analyser. Electrospray ionisation (ESI) MS spectra were recorded on a Flexar SQ 300 MS PerkinElmer

mass spectrometer. ^{1}H NMR spectra were acquired on a Bruker Avance III 400 spectrometer using DMSO-d_6 solvent. Electrochemical measurements were carried out under dinitrogen atmosphere using a CHI 6205 electrochemicalanalyser using NEt_4ClO_4 as the supporting electrolyte (0.1 mol dm^{-3}) and the solute concentration was 10^{-3} mol dm^{-3}. For electrochemical measurements a glassy carbon working electrode, Pt wire counter electrode and saturated calomel electrode (SCE) were used. The half-wave potential E_{298}^{o} was set equal to 0.5(E_{pa} +E_{pc}), where E_{pa} and E_{pc} are anodic and cathodic cyclic voltammetric peak potentials, respectively. In this cell, Fc/Fc^{+} couple had an $E_{1/2}$ value of 0.26 V. Fluorescence measurements were conducted using Fluoromax 4P spectrofluorimeter (Horiba Jobin Mayer, USA). Viscosity measurements were carried using Ostwald Viscometer at 27^{o}C.

Crystallography

Single crystals were grown by slow evaporation of [**1**]Cl in dichloromethane, [**3**]$(ClO_4)_2$ in water and [**4**]$(PF_6)(NO_3)$ in methanol. Single crystal X-ray structural studies were performed on a CCD Agilent Technologies (Oxford Diffraction) SUPER NOVA diffractometer for [**1**]Cl and [**3**]$(ClO_4)_2$ and Bruker D8 venture for [**4**]$(PF_6)(NO_3)$. Data were collected using Cu K_α (λ_α = 1.54180 Å) at 293 (2) K for [**1**]Cl and using Mo K_α radiation (λ_α = 0.71073 Å) for [**3**]$(ClO_4)_2$ and [**4**]$(PF_6)(NO_3)$ at 293(2) K and 296(2) K, respectively. The strategy for the data collection was evaluated by using the CrysAlisPro CCD software for both [**1**]Cl and [**3**]$(ClO_4)_2$ and APEX 10 software for [**4**]$(PF_6)(NO_3)$. The data were collected by the standard 'phi-omega′ scan techniques and were scaled and reduced using CrysAlisPro RED software for [**1**]Cl and [**3**]$(ClO_4)_2$ and Bruker SAINT and XPREP software for [**4**]$(PF_6)(NO_3)$. The structures were solved by direct methods using SHELXS-2013 and refined by full matrix least-squares with SHELXL-2013,

refining on F^2.[22] The positions of all the atoms were obtained by direct methods. All non-hydrogen atoms were refined anisotropically. The remaining hydrogen atoms were placed in geometrically constrained positions and refined with isotropic temperature factors, generally $1.2U_{eq}$ of their parent atoms.

CCDC reference numbers for [**1**]Cl, [**3**]$(ClO_4)_2$ and [**4**]$(PF_6)(NO_3)$ are 977269, 977270 and 977271, respectively.

Fluorescence titration: A tris-HCl buffer (pH 7.4) solution containing CT DNA (10 μM) and EB (0.33 μM) was titrated with complexes [**1**](ClO_4) - [**4**]$(PF_6)_2$ (5 mM). The mixture was shaken and waited for 10 minutes at 25^{o}C before acquiring the readings. The emission spectra were recorded from 530 nm - 700 nm with an excitation wavelength at 520 nm.

Viscosity measurements: The viscosity of CT DNA (200 μM) in presence and absence of complexes [**1**](ClO_4) - [**4**]$(PF_6)_2$ was measured in tris-HCl buffer solution (pH 7.4) at 27 ^{o}C using Ostwald Viscometer. The concentration of the complexes in the CT DNA solution was increased by an amount of 10 μM till the difference between two consecutive measurements was observed. An average of three measurements of flow time were taken and the results were presented as $(\eta/\eta_o)^{1/3}$ versus [complex]/[CT DNA], where η and η_o represents the viscosity of CT DNA solution in the presence and absence of complexes, respectively. The equation $\eta = (t - t_o)/t_o$ was employed for the calculation of viscosities where t represents the flow time CT DNA solution in the presence and absence of complexes and t_o is the flow time of buffer alone.

Bacterial Strains: *E.coli*BL21 (DE3), BL21 (DE3)-pLySS (chloramphenicol resistant), BL21 (DE3) containing pET28a (kanamycin resistant), BL21 (DE3) containing pET11a (ampicillin resistant) and *B.subtilis*168 were used in this study to determine the antibacterial activity of [**1**](ClO_4) - [**4**]$(PF_6)_2$.

Growth curve: Effects of complexes [**1**](ClO_4) - [**4**]$(PF_6)_2$ on growth curve of *E. coli* and *B. subtilis* were monitored. Overnight culture of *E.coli* and *B.subtilis* were prepared and diluted to 0.1 OD_{600}. The growth of bacteria was monitored in the presence 200 µg/mL of complexes at every one hour by reading the OD_{600} using Thermo Varioskan flash plate reader. Bacterial strain containing only DMF was taken as the control. Only LB was taken as the blank and subtracted from the all readings. Growth curve was plotted as time *vs* OD_{600}.

Disc diffusion assay: Overnight culture of different bacterial strains were prepared and diluted to OD_{600}~0.1. Three milliliter of the diluted culture was equally spread over the LB agar plates and dried for 10 minutes. Filter paper discs (0.5 cm diameter) were placed on the agar plate. Twenty five microliter of DMF containing 100 µg of complexes [**1**](ClO_4) - [**4**]$(PF_6)_2$ were placed on the discs, 25µL of DMF was used as the control and grown for 12 h at 37 ^oC.

Determination of MIC: The MIC was determined as previously described in the CLSI protocol (2012) with slight modifications. Equal number of Bacteria (5×10^5) were grown for 16 h at 37^oC in the LB medium containing different concentrations of complexes [**1**](ClO_4) - [**4**]$(PF_6)_2$ (2.5 to 1000 µg/mL). Bacterial growth was monitored by OD_{600}. MIC was noted at the lowest concentration point where no growth was observed.

Fluorescence staining and microscopy: Overnight cultures of *E. coli* and *B. subtilis* were diluted to an OD_{600} ~0.1 and grown at 37 °C. For membrane staining FM4-64 (1µM) was added to the culture at mid log phase and grown for 20 minutes at 37^oC. Cells were collected by

centrifugation, washed and resuspended in 25mM PIPES buffer of pH 7.4. Nucleoid staining was done by adding DAPI (1 μg/mL) or PI (5 μg/mL) to the cells. Cells were washed three times with PIPES buffer and 3 μL of the sample was used for microscopy. Fluorescence and DIC images were taken with Olympus BX-5 fluorescence microscope.

Electrophoretic mobility shift assay: Binding of complexes [**3**]$(ClO_4)_2$ and [**4**]$(PF_6)_2$ to the DNA was shown by shift in the electrophoretic mobility of 267 bp DNA on an agarose gel. DNA (267bp) was incubated with complexes [**3**]$(ClO_4)_2$ and [**4**]$(PF_6)_2$ for 5 minutes at room temperature and run on a 2% agarose gel and the DNA band shift was monitored.

Restriction digestion assay: PZs green plasmid vector was used for the restriction digestion assay. The plasmid vector was digested using NdeI restriction enzyme in the absence or presence of complexes [**3**]$(ClO_4)_2$ and [**4**]$(PF_6)_2$ using manufacturer's protocol. The restriction digestion was monitored on 1% agarose gel.

Preparation of metal complexes

Synthesis of [(*p*-cym)RuCl(bpmo)]ClO_4{[**1**](ClO_4)}. The starting complex [(*p*-cym)RuCl(μ-Cl)]$_2$ (50 mg, 0.069 mmol) and bpmo (48 mg, 0.15 mmol) were dissolved in 30 cm^3 methanol and heated to reflux for 6 h under aerobic condition. The initial yellow solution gradually changed to deep orange during the course of the reaction. The solvent was then removed under reduced pressure. The oily mass obtained was then dissolved in acetonitrile (~2 cm^3) and to that an aqueous solution of saturated $NaClO_4$ was added which gave brownish yellow precipitate. Filtration, followed by washing with cold water and drying under air yielded pure brownish solid {[**1**](ClO_4)}.Yield: 59 mg (58%). Anal. Calc.: C, 49.48; H, 5.19; N, 8.25. Found: C, 48.75; H, 5.32; N, 8.18. Molar conductivity [$\Lambda_M/(\Omega^{-1}$ cm^2 dm^3 $mol^{-1})$] in acetonitrile: 128. The positive ion electrospray mass spectrum of [**1**](ClO_4) in methanol exhibited the molecular ion peak centred at

m/z value of 581.27, corresponding to $\{[\mathbf{1}](ClO_4) - ClO_4\}^+$ (calculated molecular mass 581.13). ^{1}H NMR: (400 MHz, $(CD_3)_2SO$, 298 K): δ(ppm): 0.50 (m, 1H, CH-*p*-cym), 0.73 (d, J = 8Hz, 6H, $(CH_3)_2$CH-*p*-cym), 1.15 (s, 3H, CH_3-*p*-cym), 2.04(s, 6H, CH_3-pz), 2.49 (s, 6H, CH_3-pz), 3.65 (s, 3H, OCH_3), 5.73 (broad, 4H, Ar-*p*-cym), 6.24 (d, J = 8 Hz, 1H, Ar-ani), 6.35 (s, 2H, CH-pz), 7.07 (t, J = 8 Hz, 1H, Ar-ani), 7.11 (d, J = 8.0 Hz, 1H, Ar-ani), 7.50 (t, J = 8 Hz, 1H, Ar-ani), 7.59 (s, 1H, CH-$(pz)_2$). λ_{max}/nm (ε/dm^3 mol^{-1} cm^{-1}) in acetonitrile: 420 (520), 322 (3100), 283 (6030), 247 (8800), 204 (30100).

Synthesis of [(*p*-cym)RuCl(bpms)](PF$_6$) $\{[\mathbf{2}](PF_6)\}$. A mixture of [(*p*-cym)RuCl(μ-Cl)]$_2$ (50 mg, 0.083 mmol) and bpms (55 mg, 0.168 mmol) were dissolved in 30 cm^3 methanol and the mixture was heated to reflux for 6 h under aerobic condition. After completion of reaction the solvent was reduced to 2 cm^3 under vacuum and saturated solution of aqueous KPF_6 was added to it and kept in refrigerator overnight. The deep yellow precipitate obtained was filtered off and washed thoroughly with cold water and methanol and dried under vacuum which gave pure $\{[\mathbf{2}](PF_6)\}$.Yield: 84.0 mg (80%). Anal. Calc.: C, 45.31; H, 4.89; N, 7.55. Found: C, 44.90; H, 4.78; N, 7.34. Molar conductivity [Λ_M/(Ω^{-1} cm^2 dm^3 mol^{-1})] in acetonitrile: 122. The positive ion electrospray mass spectrum of $[\mathbf{2}](PF_6)$ in methanol exhibited signals centred at *m/z* values of 597.24 corresponding to $\{[\mathbf{2}](PF_6)\} - PF_6\}^+$ (calculated molecular masses are 597.20). ^{1}H NMR: (400 MHz, $(CD_3)_2SO$, 298 K): δ(ppm):0.95 (d, J = 8.0 Hz, 6H, $(CH_3)_2$CH-*p*-cym), 1.43 (m, 1H, CH-*p*-cym), 1.91 (s, 3H, CH_3-*p*-cym), 2.44(s, 3H, SCH_3), 2.49 (s, 6H, CH_3-pz), 2.50 (s, 6H, CH_3-pz), 5.34 (broad, 2H, Ar-*p*-cym), 5.66 (broad, 2H, Ar-*p*-cym), 6.24 (d, J = 8.0 Hz, 1H, Ar-thioani), 6.37 (s, 2H, CH-pz), 7.30 (t, J = 8 Hz, 1H, Ar-thioani), 7.43 (d, J = 8.0 Hz, 1H, Ar-thioani), 7.52 (t, J = 8.0 Hz, 1H, Ar-thioani), 7.62 (s, 1H, CH-$(pz)_2$). λ_{max}/nm (ε/dm^3 mol^{-1} cm^{-1}) in acetonitrile: 416 (600), 325 (2100), 295 (2960), 255 (14800), 215 (29000).

Synthesis of [(*p*-cym)Ru(H$_2$O)(bpmo)](ClO$_4$)$_2${[**3**](ClO$_4$)$_2$}. Complex {[**1**](ClO$_4$)} (50 mg, 0.063 mmol) was initially dissolved in 10 cm^3 of 1:1 methanol-water mixture and to it excess AgClO$_4$ (32 mg, 0.158 mmol) was added. The reaction mixture was stirred at ambient temperature for 3 h and then filtered through celite to remove AgCl precipitate. The volume of the solution was reduced to one fourth and to it a saturated solution of NaClO$_4$ in 1:1 methanol-water mixture was added. The solution was then kept at low temperature to yield orange colored crystals. The crystals thus formed was filtered and washed with cold water followed by cold methanol and then dried under vacuum to yield pure {[**3**](ClO$_4$)$_2$}. Yield: 30 mg (62%). Anal. Calc.: C, 44.10; H, 5.02; N, 7.35. Found: C, 43.83; H, 4.76; N, 8.04. Molar conductivity [Λ_M/(Ω^{-1} cm^2 dm^3 mol^{-1})] in acetonitrile: 198. The positive ion electrospray mass spectrum of [**3**](ClO$_4$)$_2$ in methanol exhibited the signals centred at *m/z* values of 645.10 corresponding to {{[**3**](ClO$_4$)$_2$ – ClO$_4$ – H$_2$O}$^+$ (calculated molecular mas 645.13). ^{1}H NMR: (400 MHz, (CD$_3$)$_2$SO, 298 K): δ(ppm): 0.31 (m, 1H, CH-*p*-cym), 0.72 (d, *J* = 8.0 Hz, 6H, (CH$_3$)$_2$CH-*p*-cym), 1.92 (s, 3H, CH$_3$-*p*-cym), 2.52 (s, 6H, CH$_3$-pz), 2.63 (s, 6H, CH$_3$-pz), 3.66 (s, 3H, OCH$_3$), 5.81 (broad, 2H. Ar-*p*-cym), 6.07 (d, *J* = 4.0 Hz, 2H, Ar-*p*-cym), 6.25 (d, *J* = 8.0 Hz, 1H, Ar-ani), 6.58 (s, 2H, CH-pz), 7.06 (t, *J* = 4.0 Hz, 1H, Ar-ani), 7.13 (d, *J* = 8.0 Hz, 1H, Ar-ani), 7.51 (t, *J* = 8.0 Hz, 1H, Ar-ani), 7.71 (s, 1H, CH-(pz)$_2$). λ_{max}/nm (ε/dm^3 mol^{-1} cm^{-1}) in acetonitrile: 394 (400), 318 (830), 275 (2700), 227 (10000).

Synthesis of [(*p*-cym)Ru(H$_2$O)(bpms)](PF$_6$)$_2${[**4**](PF$_6$)$_2$}.Complex {[**2**](PF$_6$)} (50 mg, 0.046 mmol) was dissolved in 10 cm^{3}1:1 methanol-water mixture and to it excess AgNO$_3$ (78mg, 0.46mmol) was added and stirred for 4 h at ambient temperature. It was then filtered through

celite to remove AgCl precipitate. The solution was then concentrated and saturated solution of KPF_6 in 1:1 methanol-water mixture was added to it and kept in refrigerator for 3 h which gave brownish yellow precipitate. The precipitate was filtered and washed carefully with cold water to remove the excess KPF_6 and dried under vacuum to get pure {[**4**]$(PF_6)_2$}.Yield 20 mg (38%). Anal. Calc.: C, 41.19; H, 4.29; N, 6.44. Found: C, 40.92; H, 4.59; N, 7.07. Molar conductivity [$\Lambda_M/(\Omega^{-1}$ cm^2 dm^3 mol^{-1})] in acetonitrile: 242. The positive ion electrospray mass spectrum of {[**4**]$(PF_6)_2$} in methanol exhibited the signal centred at *m/z* value of 723.94 corresponding to {[**4**]$(PF_6)_2$} – PF_6}$^+$ (calculated molecular mass 724.73). ^{1}H NMR: (400 MHz, $(CD_3)_2SO$, 298 K): δ(ppm): 0.94 (d, *J*= 8.0 Hz, 6H, $(CH_3)_2$CH-*p*-cym), 1.18 (m, 1H, CH-*p*-cym), 1.73 (s, 3H, CH_3-*p*-cym), 2.44 (s, 6H, CH_3-pz), 2.55 (s, 3H, SCH_3),2.64 (s, 6H, CH_3-pz), 5.92 (broad, 4H. Ar-*p*-cym), 6.19 (d, *J* = 8.0 Hz, 1H, Ar-thioani), 6.61 (s, 2H, CH-pz), 7.30 (t, *J* = 8.0 Hz, 1H, Ar-thioani), 7.42 (d, *J* = 8.0 Hz, 1H, Ar-thioani), 7.49 (t, *J* = 8.0 Hz, 1H, Ar-thioani), 7.71 (s, 1H, CH-$(pz)_2$). λ_{max}/nm (ε/dm^3 mol^{-1} cm^{-1}) in acetonitrile: 392 (590), 322 (1750), 292 (2900), 259 (9300), 238 (18000), 213 (28300).

Acknowledgements

Authors are thankful to the Department of Science and Technology (SR/S1/IC-20/2010), Govt. of India and Indian Institute of Technology, Bhubaneswar (GP03) for financial support. SKT, ND and AS are grateful to CSIR, UGC and DST (inspire programme), New Delhi, India for fellowship. The authors acknowledge Professor S. Chatterjee, National Institute of Technology, Rourkela, India for recording ^{1}H NMR and Mass spectra of the complexes. The authors would

also like to thank the reviewers for their valuable comments and suggestions to improve the manuscript.

References

1 (a) H. W. Boucher, G. H. Talbot, J. S. Bradley, J. E. Edwards, D. Gilbert, L. B. Rice, M. Scheld, B. Spellberg and J. Bartlett, *Clin. Infect. Dis.,* 2009, **48**, 1-12; (b) P. L. Lam, G. L. Lu, K. M. Hon, K. W. Lee, C. L. Ho, X. Wang, J. C. O. Tang, K. H. Lam, R. S. M. Wong, S. H. L. Kok, Z. X. Bian, H. Li, K. K. H. Lee, R. Gambari, C. H. Chui and W. Y. Wong, *Dalton Trans.,* 2014, **43**, 3949-3957; (c) M. D. King, B. J. Humphrey, Y. F. Wang, E. V. Kourbatova, S. M. Ray and H. M. Blumberg, *Ann. Intern. Med.,* 2006, **144**, 309-317; (d) R. Klevens, M. A. Morrison, J. Nadle and et al., *J. Am. Med. Assoc.,* 2007, **298**, 1763-1771; (e) K. E. Jones, N. G. Patel, M. A. Levy, A. Storeygard, D. Balk, J. L. Gittleman and P. Daszak, *Nature,* 2008, **451**, 990-U994; f) P. J. Vikesland and K. R. Wigginton, *Environ. Sci. Tech.,* 2010, **44**, 3656-3669.

2 (a) K. M. G. O'Connell, J. T. Hodgkinson, H. F. Sore, M. Welch, G. P. C. Salmond and D. R. Spring, *Angew. Chem. Int. Ed.,* 2013, **52**, 10706-10733; (b) J. Y. Zhang, Y. P. Chen, K. P.

Miller, M. S. Ganewatta, M. Bam, Y. Yan, M. Nagarkatti, A. W. Decho and C. B. Tang, *J. Am. Chem. Soc.,* 2014, **136**, 4873-4876.

3 (a) J. A. Lemire, J. J. Harrison and R. J. Turner, *Nat. Rev. Micro.,* 2013, **11**, 371-384; (b) K.-H. Choi, H.-J. Lee, B. J. Park, K.-K. Wang, E. P. Shin, J.-C. Park, Y. K. Kim, M.-K. Oh and Y.-R. Kim, *Chem. Commun.,* 2012, **48**, 4591-4593; (c) M. Wenzel, M. Patra, C. H. Senges, I. Ott, J. J. Stepanek, A. Pinto, P. Prochnow, C. Vuong, S. Langklotz, N. Metzler-Nolte and J. E. Bandow, *ACS Chem. Biol.,* 2013, **8**, 1442-1450; (d) J. Kljun, A. J. Scott, T. L. Rizner, J. Keiser and I. Turel, *Organometallics,* 2014, **33**, 1594-1601.

4 (a) W.-Y. Wong, *Coord. Chem. Rev.,* 2005, **249**, 971-997; (b) A. M. Elsome, J. M. T. Hamilton-Miller, W. Brumfitt and W. C. Noble, *J. Antimicro. Chemother.,* 1996, **37**, 911-918; (c) E. L. Chang, C. Simmers and D. A. Knight, *Pharmaceuticals,* 2010, **3**, 1711-1728; (d) M. Patel, M. Chhasatia and P. Parmar, *Eur. J. Med. Chem.,* 2010, **45**, 439-446; (e) A. A. Massoud, V. Langer, Y. M. Gohar, M. A. M. Abu-Youssef, J. Janis, G. Lindberg, K. Hansson and L. Ohrstrom, *Inorg. Chem.,* **2013**, *52*, 4046-4060; (f) I. Turel, *Coord. Chem. Rev.,* 2002, **232**, 27-47.

5 A. Bolhuis, L. Hand, J. E. Marshall, A. D. Richards, A. Rodger and J. Aldrich-Wright, *Eur. J. Pharm. Sci.,* 2011, **42**, 313-317.

6 (a) S. K. Tripathy, R. K. Surada, R. K. Manne, S. M. Mobin, M. K. Santra and S. Patra, *Dalton Trans.,* 2013, **42**, 14081-14091; (b) H. K. Liu and P. J. Sadler, *Acc. Chem. Res.,* 2011, **44**, 349-359; (c) F. Lentz, A. Drescher, A. Lindauer, M. Henke, R. A. Hilger, C. G. Hartinger, M. E. Scheulen, C. Dittrich, B. K. Keppler, U. Jaehde and E. Central European Society for Anticancer Drug Research, *Anticancer Drugs,* 2009, **20**, 97-103; (d) I. Bratsos, G. Birarda, S. Jedner, E. Zangrando and E. Alessio, *Dalton Trans.,* 2007, 4048-4058; (e) R. A. Adigun, B.

Martincigh, V. O. Nyamori, B. Omondi, C. Masimirembwa and R. H. Simoyi, *Dalton Trans.,* 2014, **43**, 12943-12951; (f) S. Pillozzi, L. Gasparoli, M. Stefanini, M. Ristori, M. D'Amico, E. Alessio, F. Scaletti, A. Becchetti, A. Arcangeli and L. Messori, *Dalton Trans.,* 2014, **43**, 12150-12155; (g) P. Chellan, K. M. Land, A. Shokar, A. Au, S. H. An, D. Taylor, P. J. Smith, T. Riedel, P. J. Dyson, K. Chibale and G. S. Smith, *Dalton Trans.,* 2014, **43**, 513-526; (h) S. K. Tripathy, U. De, N. Dehury, S. Pal, H. S. Kim and S. Patra, *Dalton Trans.,* 2014, **43**, 14546-14549.

7 (a) F. Li, Y. Mulyana, M. Feterl, J. M. Warner, J. G. Collins and F. R. Keene, *Dalton Trans.,* 2011, **40**, 5032-5038; (b) F. R. Keene, *Dalton Trans.,* 2011, **40**, 2405-2418; (c) Y. Mulyana, D. K. Weber, D. P. Buck, C. A. Motti, J. G. Collins and F. R. Keene, *Dalton Trans.,* 2011, **40**, 1510-1523; (d) A. K. Gorle, M. Feterl, J. M. Warner, L. Wallace, F. R. Keene and J. G. Collins, *Dalton Trans.,* 2014, **43**, 16713-16725; (e) Y. Li, C. de Kock, P. J. Smith, H. Guzgay, D. T. Hendricks, K. Naran, V. Mizrahi, D. F. Warner, K. Chibale and G. S. Smith, *Organometallics,* 2012, **32**, 141-150.

8 (a) R. K. Gupta, G. Sharma, R. Pandey, A. Kumar, B. Koch, P. Z. Li, Q. Xu and D. S. Pandey, *Inorg. Chem.,* 2013, **52**, 13984-13996; (b) R. P. Paitandi, R. K. Gupta, R. S. Singh, G. Sharma, B. Koch and D. S. Pandey, *Eur. J. Med. Chem.,* 2014, **84**, 17-29; (c) A. Levina and P. A. Lay, *Inorg. Chem. Front.,* 2014, **1**, 44-48; (d) A. Vergara, G. D'Errico, D. Montesarchio, G. Mangiapia, L. Paduano and A. Merlino, *Inorg. Chem.,* 2013, **52**, 4157-4159; (e) F. Li, M. Feterl, J. M. Warner, A. I. Day, F. R. Keene and J. G. Collins, *Dalton Trans.,* 2013, **42**, 8868-8877; (f) N. Busto, J. Valladolid, M. Martinez-Alonso, H. J. Lozano, F. A. Jalon, B. R. Manzano, A. M. Rodriguez, M. C. Carrion, T. Biver, J. M. Leal, G. Espino and B. Garcia, *Inorg. Chem.,* 2013, **52**, 9962-9974.

9 (a) N. Dehury, S. K. Tripathy, A. Sahoo, N. Maity and S. Patra, *Dalton Trans.,* 2014, **43**, 16597-16600; (b) F. Marchetti, C. Pettinari, R. Pettinari, A. Cerquetella, C. Di Nicola, A. Macchioni, D. Zuccaccia, M. Monari and F. Piccinelli, *Inorg. Chem.,* 2008, **47**, 11593-11603; (c) S. Betanzos-Lara, Z. Liu, A. Habtemariam, A. M. Pizarro, B. Qamar and P. J. Sadler, *Angew. Chem. Int. Ed. Engl.,* 2012, **51**, 3897-3900; (d) Y. Borguet, X. Sauvage, G. Zaragoza, A. Demonceau and L. Delaude, *Organometallics,* 2011, **30**, 2730-2738; (e) C. Aliende, M. Pérez-Manrique, F. A. Jalón, B. R. Manzano, A. M. Rodríguez and G. Espino, *Organometallics,* 2012, **31**, 6106-6123; (f) G. Süss-Fink, *J. Organomet. Chem.,* 2014, **751**, 2-19; (g) P. Kumar, R. K. Gupta and D. S. Pandey, *Chem. Soc. Rev.,* 2014, **43**, 707-733.

10 Z. Adhireksan, G. E. Davey, P. Campomanes, M. Groessl, C. M. Clavel, H. Yu, A. A. Nazarov, C. H. F. Yeo, W. H. Ang, P. Dröge, U. Rothlisberger, P. J. Dyson and C. A. Davey, *Nat. Commun.,* **2014**, *5*.

11 (a) F. F. Li, M. Feterl, Y. Mulyana, J. M. Warner, J. G. Collins and F. R. Keene, *J. Antimicro. Chemother.,* 2012, **67**, 2686-2695; (b) M. Pandrala, F. Li, M. Feterl, Y. Mulyana, J. M. Warner, L. Wallace, F. R. Keene and J. G. Collins, *Dalton Trans.,* 2013, **42**, 4686-4694; (c) F. Li, M. Feterl, J. M. Warner, F. R. Keene and J. G. Collins, *J. Antimicro. Chemother.,* 2013, **68**, 2825-2833.

12 M. Adams, Y. Li, H. Khot, C. De Kock, P. J. Smith, K. Land, K. Chibale and G. S. Smith, *Dalton Trans.,* 2013, **42**, 4677-4685.

13 (a) I. Turel, J. Kljun, F. Perdih, E. Morozova, V. Bakulev, N. Kasyanenko, J. A. W. Byl and N. Osheroff, *Inorg. Chem.,* 2010, **49**, 10750-10752; (b) R. Hudej, J. Kljun, W. Kandioller, U. Repnik, B. Turk, C. G. Hartinger, B. K. Keppler, D. Miklavčič and I. Turel, *Organometallics,*

2012, **31**, 5867-5874; (c) J. Kljun, A. K. Bytzek, W. Kandioller, C. Bartel, M. A. Jakupec, C. G. Hartinger, B. K. Keppler and I. Turel, *Organometallics,* 2011, **30**, 2506-2512.

14 T. J. Morin, B. Bennett, S. V. Lindeman and J. R. Gardinier, *Inorg. Chem.,* 2008, **47**, 7468-7470.

15 M. C. Carrion, F. Sepulveda, F. A. Jalon, B. R. Manzano and A. M. Rodriguez, *E. J. Inorg. Chem.,* 2013, 217-227.

16 (a) S. K. Tripathy, R. K. Surada, R. K. Manne, S. M. Mobin, M. K. Santra and S. Patra, *Dalton Trans.,* 2013, **42**, 14081-14091; (b) A. K. Singh, M. Yadav, R. Pandey, P. Kumar and D. S. Pandey, *J. Organomet. Chem.,* 2010, **695**, 1932-1939; (c) P. Govindaswamy, B. Therrien, G. Süss-Fink, P. Štěpnička and J. Ludvík, *J. Organomet. Chem.,* 2007, **692**, 1661-1671.

17 N. Chanda, S. M. Mobin, V. G. Puranik, A. Datta, M. Niemeyer and G. K. Lahiri, *Inorg. Chem.,* 2004, **43**, 1056-1064.

18 A. Das, T. M. Scherer, A. D. Chowdhury, S. M. Mobin, W. Kaim and G. K. Lahiri, *Inorg. Chem.,* 2012, **51**, 1675-1684.

19 M. C. Carrión, F. Sepúlveda, F. A. Jalón, B. R. Manzano and A. M. Rodríguez, *Organometallics,* 2009, **28**, 3822-3833.

20 (a) X. -B. Fu, J. -J. Zhang, D. -D. Liu, Q. Gan, H. W. Gao, Z. W. Mao and X. Y. Le, *J. Inorg. Biochem.,* 2015, **143**, 77; (b) Y. -C. Liu, Z. -F. Chen, L. -M. Liu, Y. Peng, X. Hong, B. Yang, H. -G. Liu, H. Liang and C. Orvig, *Dalton Trans.,* 2009, 10813.

21 M. A. Bennett, T. N. Huang, T. W. Matheson and A. K. Smith, *Inorg. Synth.,* 1982, **21**, 74-78.

22 G. M. Sheldrick, *Acta Crystallogr. Sect. A,* 2008, **64**, 112-122.

Table 1 Selected crystallographic data for complexes [**1**]Cl.2H_2O, [**3**]$(ClO_4)_2$ and [**4**]$(PF_6)(NO_3)$.

	[**1**]Cl.2H_2O	[**3**]$(ClO_4)_2$	[**4**]$(PF_6)(NO_3)$
emperical formula	$C_{28}H_{39}Cl_2N_4O_{2.5}Ru$	$C_{28}H_{38}Cl_2N_4O_{10}Ru$	$C_{28}H_{37}N_5O_4SPF_6Ru$
Fw	643.62	762.59	785.73
radiation	CuK_α	MoK_α	MoK_α
wavelenght	1.54180 Å	0.71073 Å	0.71073 Å
temp./ K	293 (2)	293(2)	296(2)
cryst system	Monoclinic	Triclinic	Triclinic

space group	*P 21/n*	*P*–1	*P*–1
a/Å	9.178(9)	9.5546(4)	10.3255 (8)
b/Å	17.368(17)	10.6513(5)	10.5283 (9)
c/Å	18.339(2)	15.9201(7)	15.1940 (12)
α(deg)	90.000	86.556(4)	93.340 (2)
β(deg)	93.809(11)	87.525(3)	93.375 (2)
γ(deg)	90.000	88.928(4)	95.141 (2)
V/ Å^3	2917(4)	1615.53(12)	1638.9 (2)
Crystal size	0.23 x 0.16 x 0.13 mm	0.36x0.28x0.22mm	0.34×0.24×0.20 mm
Z	4	2	2
D_{calcd} / g cm^{-3}	1.466	1.568	1.592
F(000)	1332	784	802
θ range	3.509-71.8	3.04-28.72	2.29 – 28.39
Data/restraints/parameters	5632/6/360	7299/105/451	8170/3/423
R1,wR2 [I>2σ(I)]	0.0699, 0.1826	0.0435, 0.0972	0.053, 0.1314
R1,wR2 (all data)	0.0715, 0.1840	0.0566, 0.1084	0.0753, 0.1500
Largest diff. peak hole (eÅ^{-3})	2.615/-2.159	0.557/-0.754	0.814/−0.799

Table 2 Important bond distances (Å) and bond angles (°) for [**1**]Cl.2H_2O, [**3**]$(ClO_4)_2$ and [**4**]$(PF_6)(NO_3)$.

	[**1**]Cl.2H_2O	[**3**]$(ClO_4)_2$	[**4**]$(PF_6)(NO_3)$
Ru(1)-N(1)	2.141 (4)	2.133 (2)	2.137 (3)
Ru(1)-N(3)	2.139 (5)	2.120 (2)	2.129 (3)
Ru(1)-Cl(1)/O(1)	2.427 (13)	2.141 (2)	2.125 (3)
Ru(1)-C(20)	2.249 (6)	2.237 (3)	2.219 (4)
Ru(1)-C(21)	2.194 (6)	2.173 (3)	2.178 (4)
Ru(1)-C(22)	2.206 (5)	2.165 (3)	2.199 (4)
Ru(1)-C(23)	2.255 (5)	2.209 (3)	2.223 (4)
Ru(1)-C(24)	2.221 (5)	2.206 (3)	2.180 (4)
Ru(1)-C(25)	2.224 (6)	2.194 (3)	2.211 (4)
Ru(1)-$C_{centroid}$	1.713	1.695	1.694
N(1)-Ru(1)-N(3)	84.31 (19)	85.82 (9)	85.63 (11)
N(1)-Ru(1)-Cl(1)/O(1)	83.34 (13)	78.86 (10)	79.72 (11)
N(3)-Ru(1)-Cl(1)/O(1)	85.93 (13)	82.81 (9)	84.02 (12)

Table 3 DNA binding parameters (K_{SV} and K_{app}) and antibacterial activity (MIC and zones of inhibition) of the complexes [**1**](ClO_4) – [**4**](PF_6)$_2$ against *E. coli* and *B. subtilis*.

Complexes	DNA binding profile		MIC (μg/mL)		Inhibition zone (mm)	
	K_{app} (M^{-1})	K_{SV}	*E. coli*	*B. subtilis*	*E. coli*	*B. subtilis*
[**1**](ClO_4)	4.5 x 10^4	1.1 x 10^4	1000	1000	8.6	7.4
[**2**](PF_6)	5.5 x 10^4	1.4 x 10^4	580	750	9.9	10.0
[**3**](ClO_4)$_2$	7.0 x 10^4	1.7 x 10^4	100	100	12.8	12.4
[**4**](PF_6)$_2$	9.9 x 10^4	2.0 x 10^4	30	66	14.1	14.3

Fig.1 Positive ion ESI mass spectra of complexes $\mathbf{1}^{+}$-$\mathbf{4}^{2+}$ in CH_3OH.

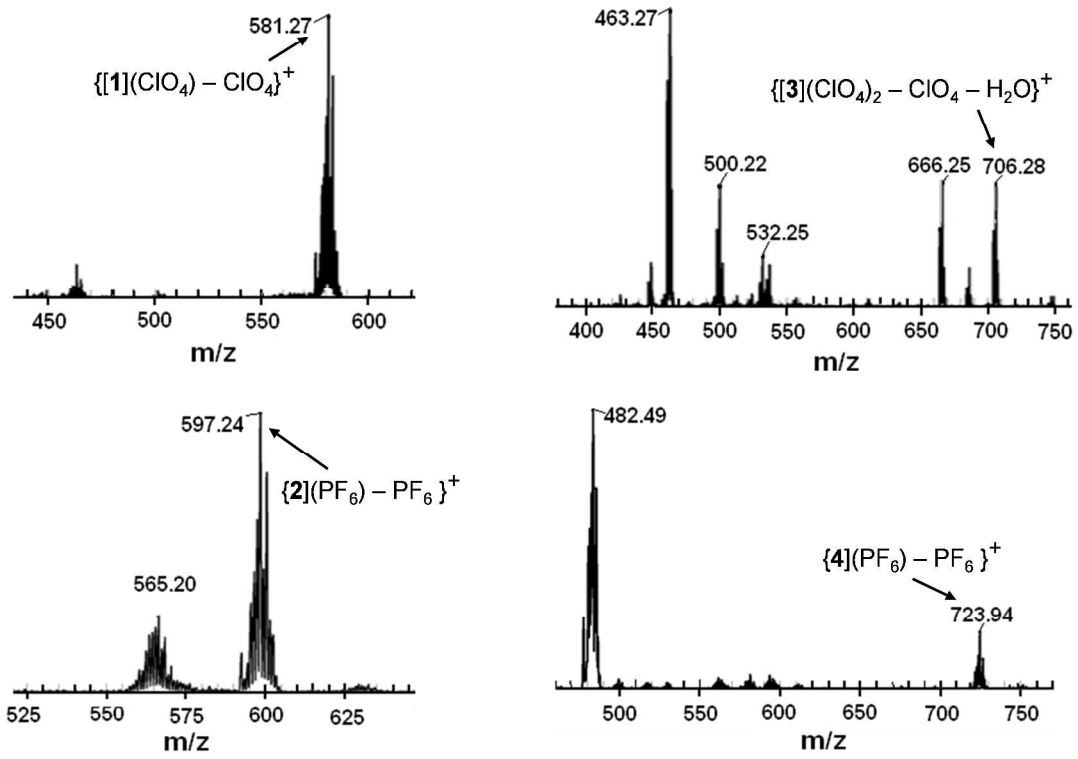

Fig. 2 ORTEP diagram of the complexes (a) [**1**](Cl).2H_2O, (b) [**3**](ClO_4)$_2$ and (c) [**4**](PF_6)(NO_3).Ellipsoids were drawn at 20% probability level. Hydrogen atoms (except O-H protons) and counter anions (Cl^-, ClO_4^-, PF_6^- and NO_3^-) are eliminated for clarity.

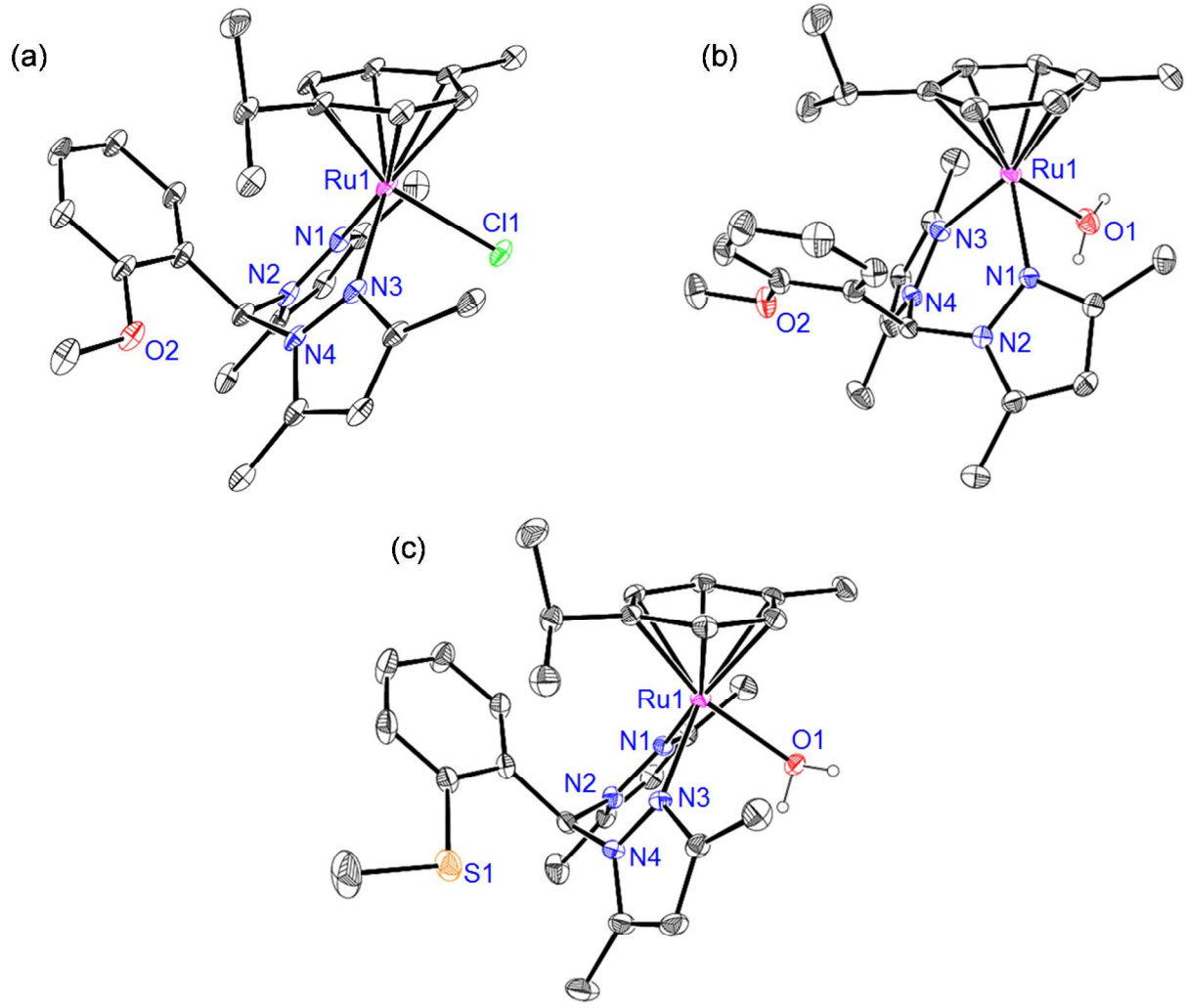

Fig. 3 Ruthenium complexes [**1**](ClO_4) - [**4**]($(PF_6)_2$ inhibit the growth of bacteria. **Panel A** shows a disc diffusion assay showing the inhibition zones of *E. coli and B. subtilis* growth on LB agar media after treatment with 100 µg of each. **Panel B** represents growth curves showing the inhibitory effects of complexes on the bacterial growth.

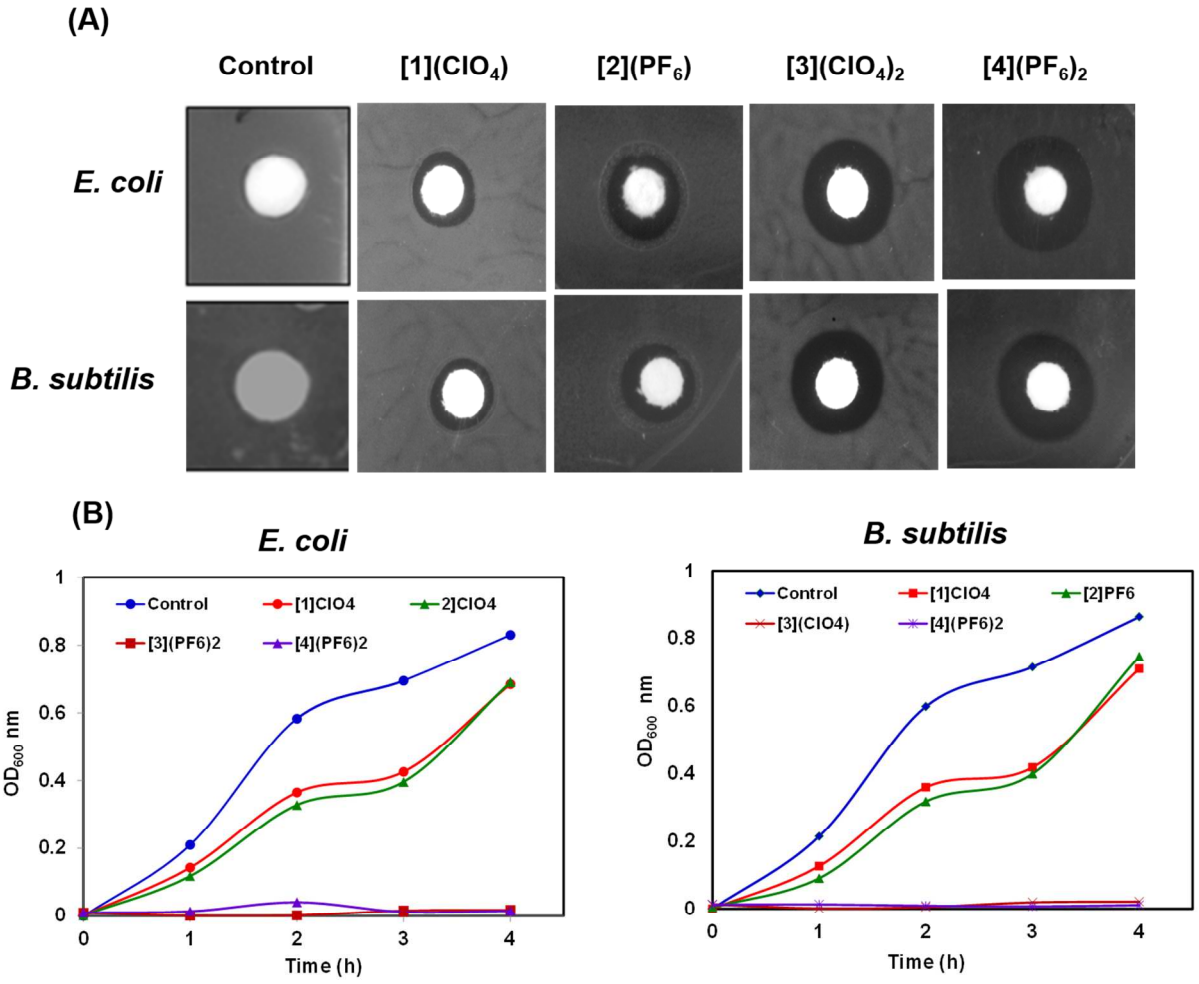

Fig. 4 Ruthenium complexes [**3**]$(ClO_4)_2$ and [**4**]$(PF_6)_2$ are active against the various resistant bacterial strains. A disk diffusion assay was performed to investigate the efficacy of the ruthenium complexes on different resistant bacterial strains. Shown are the inhibition zones formed in the presence of 100 μg of each complex.

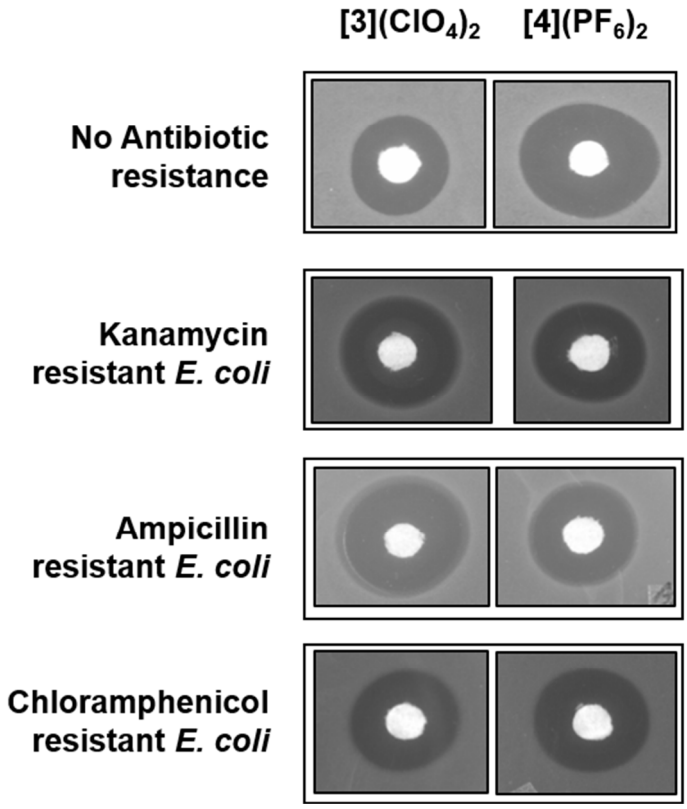

Fig. 5 Effects of the ruthenium complexes on *E. coli* (A, B) morphology and (C) nucleoid structure: *E. coli* was grown in the absence and presence of [**3**]$(ClO_4)_2$ or [**4**]$(PF_6)_2$ at MIC concentrations. Cell morphology, membrane and the nucleoid were visualized using DIC and fluorescence microscopy. ***Panel A*** shows the DIC images of *E. coli* (left column), membrane stained with FM-4-64 (middle column) and nucleoid stained with DAPI (right column), ***Panel B*** shows the DIC images (left column) and the partially lysed cells identified by staining with PI (right column) (Scale bar is 5µm).

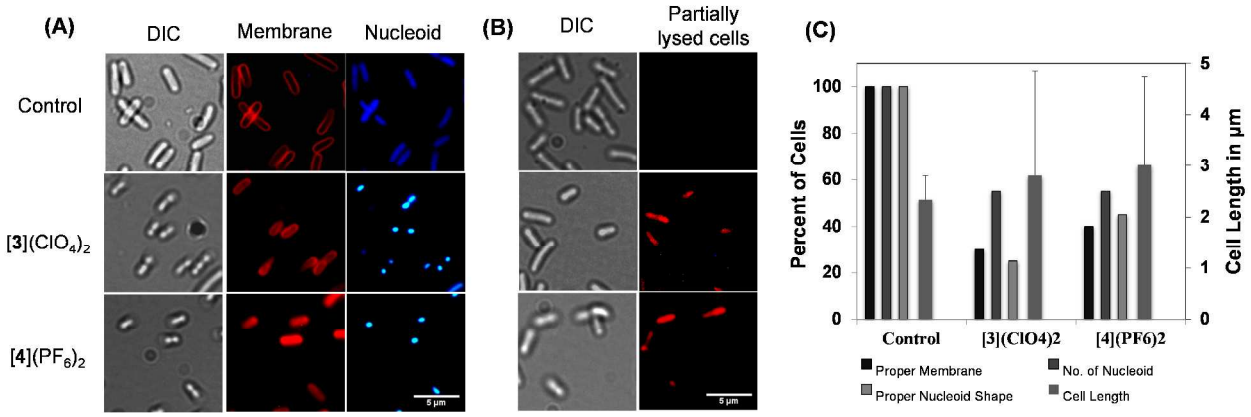

Fig. 6 DNA binding assays: Panel A, Electrophoretic mobility shift assay showing the shift of 267bp DNA upon binding to the complexes. Shown are DNA ladder (lane 1), control DNA (lane 2), DNA with 25µg of [**3**]$(ClO_4)_2$ (lane 3), DNA with 50 µg of [**3**]$(ClO_4)_2$ (lane 4), DNA with 25µg of [**4**]$(PF_6)_2$ (Lane 5) and DNA with 50µg of [**4**]$(PF_6)_2$ (Lane 6). **Panel B**, Inhibition of restriction digestion by ruthenium complexes. Shown are DNA ladder (lane 1), undigested plasmid (lane 2), plasmid digested with NdeI (lane 3) and plasmid digested with NdeI in the presence of 5µM of EB (lane 4), 10µg of [**3**]$(ClO_4)_2$ (lane 5) and 10µg of [**4**]$(PF_6)_2$ (lane 6).

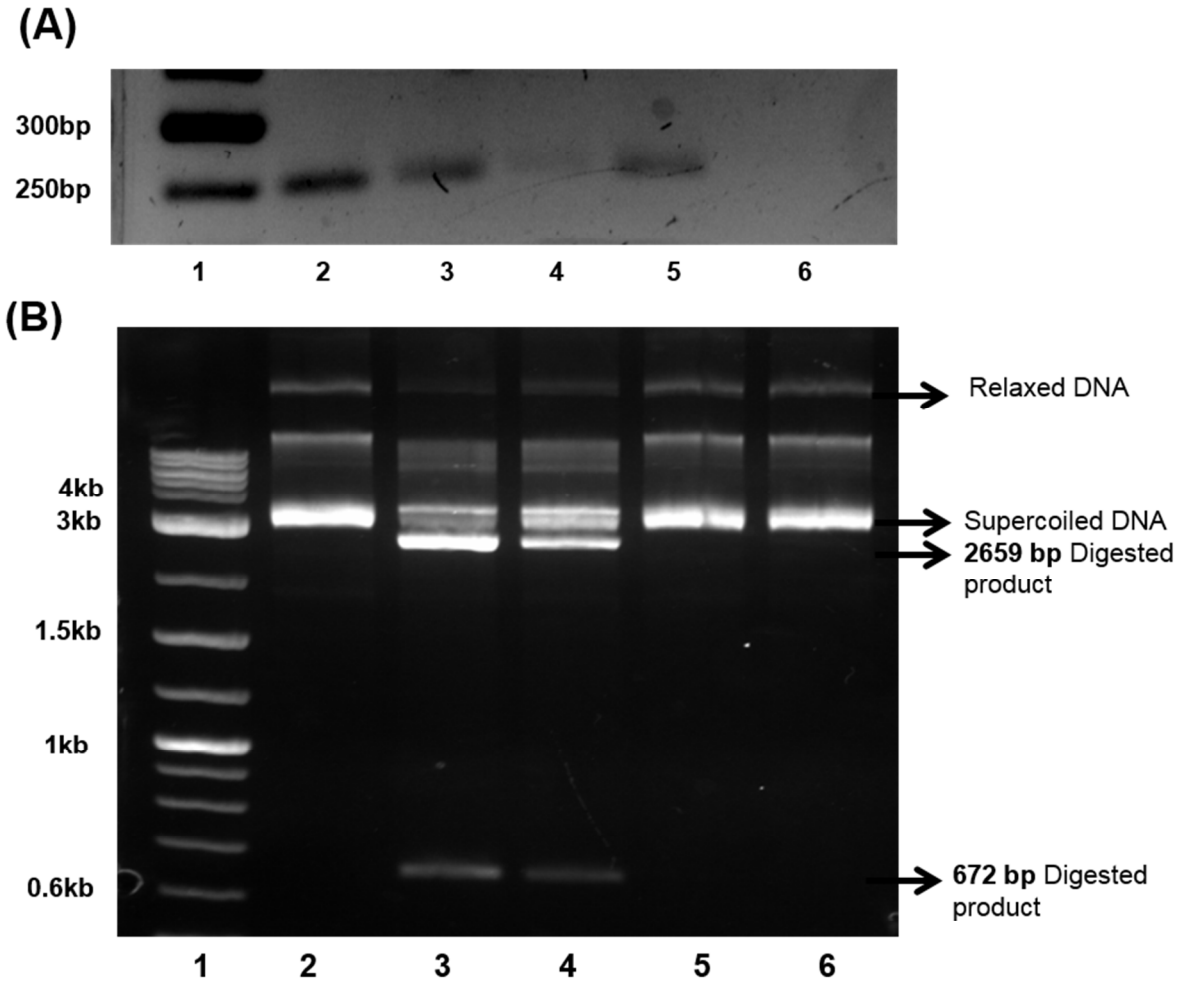

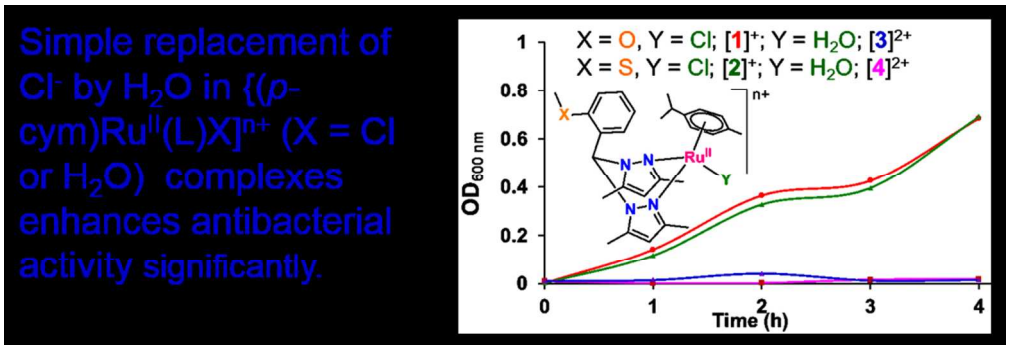

189x64mm (150 x 150 DPI)